Mutations in BRAF and KRAS Converge on Activation of the Mitogen-Activated Protein Kinase Pathway in Lung Cancer Mouse Models

Hongbin Ji,[1,2] Zhenxiong Wang,[1] Samanthi A. Perera,[1] Danan Li,[1,2] Mei-Chih Liang,[1,2]
Sara Zaghlul,[1,2] Kate McNamara,[1,2] Liang Chen,[1,2] Mitchell Albert,[3] Yanping Sun,[3]
Ruqayyah Al-Hashem,[3] Lucian R. Chirieac,[4] Robert Padera,[4] Roderick T. Bronson,[6]
Roman K. Thomas,[1,7] Levi A. Garraway,[1,7] Pasi A. Jänne,[1,5] Bruce E. Johnson,[1,5]
Lynda Chin,[1] and Kwok-Kin Wong[1,5]

[1]Department of Medical Oncology, Dana-Farber Cancer Institute; [2]Ludwig Center for Cancer Research at Dana-Farber/Harvard Cancer Center; Departments of [3]Radiology, [4]Pathology, and [5]Medicine, Brigham and Women's Hospital, Harvard Medical School; [6]Department of Pathology, Harvard Medical School, Boston, Massachusetts; and [7]The Broad Institute of MIT and Harvard, Cambridge, Massachusetts

Abstract

Mutations in the *BRAF* and *KRAS* genes occur in ∼1% to 2% and 20% to 30% of non–small-cell lung cancer patients, respectively, suggesting that the mitogen-activated protein kinase (MAPK) pathway is preferentially activated in lung cancers. Here, we show that lung-specific expression of the BRAF V600E mutant induces the activation of extracellular signal–regulated kinase (ERK)-1/2 (MAPK) pathway and the development of lung adenocarcinoma with bronchioloalveolar carcinoma features *in vivo*. Deinduction of transgene expression led to dramatic tumor regression, paralleled by dramatic dephosphorylation of ERK1/2, implying a dependency of BRAF-mutant lung tumors on the MAPK pathway. Accordingly, *in vivo* pharmacologic inhibition of MAPK/ERK kinase (MEK; MAPKK) using a specific MEK inhibitor, CI-1040, induced tumor regression associated with inhibition of cell proliferation and induction of apoptosis in these *de novo* lung tumors. CI-1040 treatment also led to dramatic tumor shrinkage in murine lung tumors driven by a mutant *KRas* allele. Thus, somatic mutations in different signaling intermediates of the same pathway induce exquisite dependency on a shared downstream effector. These results unveil a potential common vulnerability of BRAF and KRas mutant lung tumors that potentially affects rational deployment of MEK targeted therapies to non–small-cell lung cancer patients. [Cancer Res 2007;67(10):4933–9]

Introduction

The RAF family of serine/threonine kinases encompasses three members: ARAF, BRAF, and CRAF (RAF-1; ref. 1). Whereas ARAF and CRAF engage in more than one signaling pathway, mitogen-activated protein kinase (MAPK)/extracellular signal–regulated kinase (ERK) kinase (MEK)–1 and MEK-2 are the only known substrates for BRAF (1), making BRAF an ideal candidate for studying the effect of the MAPK pathway in tumorigenesis and tumor maintenance. Mutations in the *BRAF* gene were recently identified in ∼8% of human cancers whereas mutations in *ARAF* or *CRAF* seem to be rare if not nonexisting (2, 3). The most common BRAF mutation (>90%) is a valine-to-glutamate substitution at residue 600 (V600E; ref. 2), which exhibits 12.5-fold higher basal kinase activity than that of wild-type BRAF (1). In studies using NIH 3T3 cells and murine melanocytes, expression of BRAF V600E is transforming, causing constitutive ERK activation, leading to cellular proliferation, and permitting these transformed cells to grow as tumors in nude mice (1).

Whereas many oncogenic genetic lesions activate the MAPK pathway, it is unclear whether this is a necessary condition for oncogenic transformation or merely a side effect, in particular in the lung lineage. For example, MAPK pathway activation coincides with epidermal growth factor receptor (EGFR) mutant expression in *de novo* murine lung cancer driven by EGFR mutants (4–6). However, in non–small-cell lung cancer with *EGFR* kinase domain mutations, the tumors are dependent on the AKT and signal transducers and activators of transcription-3 pathways for cell survival and tumor maintenance whereas the MAPK pathway plays only a minor role (7). In addition, although multiple effector pathways including MAPK, RalGEF, and phosphatidylinositol 3-kinase/AKT are required for RAS mutants to transform cells, only the phosphatidylinositol 3-kinase/AKT pathway is responsible for tumor maintenance once the tumor microenvironment is established (8). Interestingly, inhibition of AKT-mammalian target of rapamycin pathway only reduced the size and number of early lung tumor lesions induced by KRas mutant expression whereas no apoptosis of tumor cells was observed (9), indicating that the AKT-mammalian target of rapamycin pathway likely contributes to tumor progression but not tumor maintenance in murine lung tumors with *KRas* mutation. Therefore, it is still unclear whether KRAS and BRAF mutants exert complementary or overlapping downstream effects, a finding which would be consistent with an epistatic relationship between mutations in the two oncogenes. Furthermore, the availability of inhibitors targeting different members of the MAPK pathway may help to clarify the optimal deployment and future development of these drugs (1, 10).

Recently, mice harboring a conditional knock-in allele of *BRAF* mutant using a Lox/Cre approach have been generated. This study showed that BRAF V600E mutant was able to induce several hallmarks of transformation in some primary mouse cells (11).

However, it remains unclear if BRAF mutant expression itself is sufficient to drive lung tumorigenesis *in vivo*. Here, we generated the lung cancer mouse model by inducible expression of BRAF V600E in the lung epithelial compartment. Using this model and the KRas G12D lung cancer mouse model (4–6, 12), we further investigated the potential roles of the MAPK pathway in lung tumorigenesis and tumor maintenance.

Materials and Methods

Mouse cohorts. *BRAF** mice were generated as described in Supplementary Materials and Methods. The *CCSP-rtTA* and *Ink4A/Arf*$^{-/-}$ mice were generously provided by Dr. Jeffery Whitsett (University of Cincinnati, Cincinnati, OH) and Dr. Ronald DePinho (Dana-Farber Cancer Institute, Boston, MA), respectively (12). The littermates served as controls in all the experiments. The *KRas** mice were generously provided by Drs. Katerina Politi and Harold E. Varmus (Memorial Sloan-Kettering Cancer Center, New York, NY; ref. 12). All mice were housed in a pathogen-free environment at the Dana-Farber Cancer Institute. The mice were handled in strict accord with good animal practice as defined by the Office of Laboratory Animal Welfare, and all animal work was done with DFCI Institutional Animal Care and Use Committee approval. Genotyping protocols are supplied in Supplementary Materials and Methods.

Histology and immunohistochemistry. The histology and immunohistochemistry analysis on mice lungs were done as previously described (4, 5). Details for immunohistochemistry and antibody information are provided in Supplementary Materials and Methods.

Doxycycline withdrawal and cancer therapy using MEK inhibitor *in vivo*. After sustained doxycycline treatment, the bitransgenic mice including *C/BRAF** and *C/KRas** mice were subjected to magnetic resonance imaging (MRI) to document the lung tumor burden. For doxycycline withdrawal experiment, the *C/BRAF** mice were given normal diet and MRI rescanned at indicated time points. For targeted therapies,

CI-1040 (generously provided by Pfizer, Inc.) formulated in 0.5% methocellulose-0.4% polysorbate-80 (Tween 80; Sigma-Aldrich) was given to mice including *C/BRAF** and *C/KRas** mice by gavages at 150 mg/kg twice a day. After treatment, the same mice were analyzed by MRI at different time points to determine the tumor response. The mice were sacrificed and subjected to histologic and biochemical analysis.

Reverse transcription-PCR. Total RNA samples were prepared as previously described (5) and retrotranscribed into first-strand cDNA using the SuperScript First-Strand Synthesis System following the manufacturer's protocol (Invitrogen). Additional details are provided in Supplementary Materials and Methods.

Western blot analysis. The lungs were homogenized in radioimmunoprecipitation assay buffer containing the protease inhibitor cocktails and phosphatase inhibitors (EMD Biosciences, San Diego, CA) and subjected to Western blotting. Antibody information is listed in Supplementary Materials and Methods.

MRI and tumor volume measurement. MRI measurements were done as described before (4, 5). Using the retinoic acid response element sequence scans, volume measurements of the tumors were done using in-house customized software as previously described (4, 5) and statistical analysis was done using Student's *t* test.

Results

Expression of BRAF* mutant leads to development of lung adenocarcinoma *in vivo*. We generated the *Tet-op-BRAF V600E* mice (*BRAF**; details in Supplementary Fig. S1 and Supplementary Materials and Methods) and then crossed them to *CCSP-rtTA* mice. Reverse transcription-PCR (RT-PCR) was done to detect the transgene expression in the lungs from *CCSP-rtTA/Tet-op-BRAF V600E* mice (hereinafter referred to as *C/BRAF**) before and after doxycycline administration. As predicted, no transgene
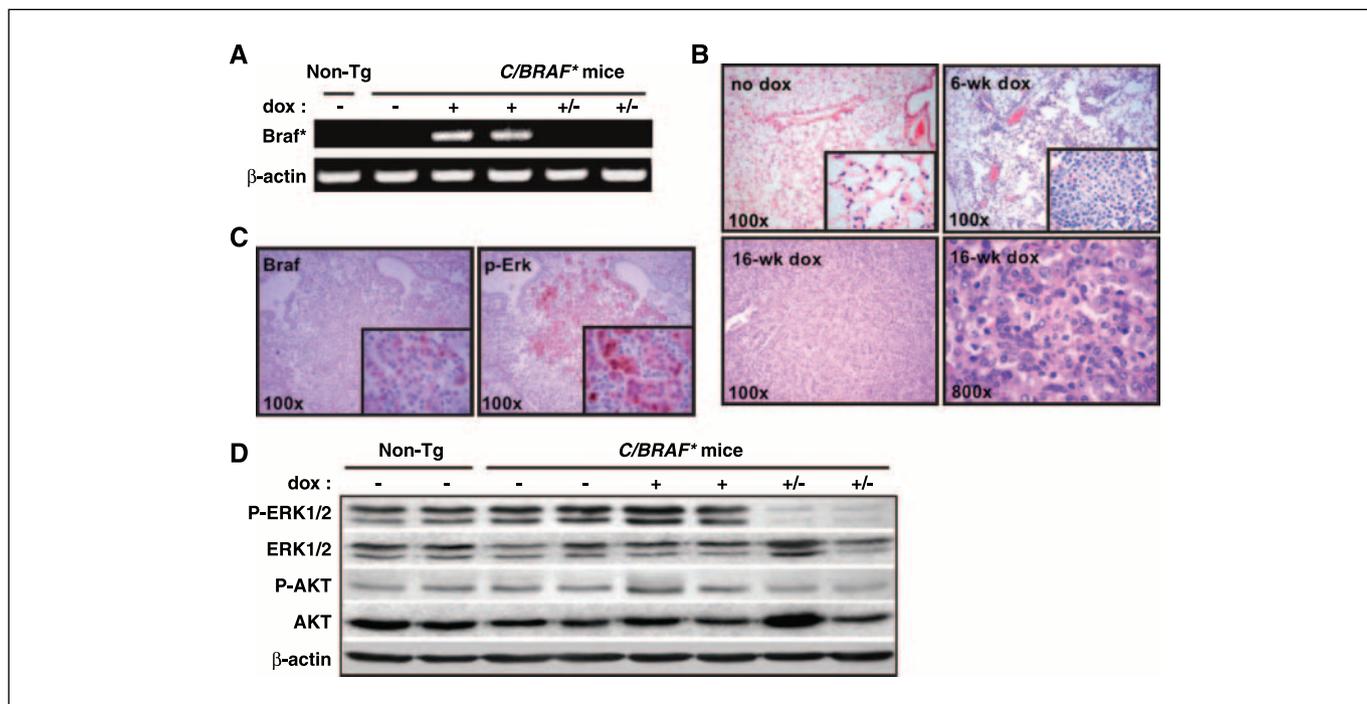

Figure 1. Inducible expression of BRAF* in the bitransgenic *C/BRAF** mice lung epithelium leads to MAPK activation and lung adenocarcinoma development. *A*, RT-PCR analyses of the induction or deinduction of *BRAF** transgene transcription in the lungs of *C/BRAF** mice after 12 wk of doxycycline administration (+) and/or followed by 2 wk of doxycycline withdrawal (+/−). Nontransgenic mice serve as negative control. The endogenous β-actin transcription levels serve as control. *B*, histologic analysis of lungs from *C/BRAF** mice with or without doxycycline treatment for indicated time. *C*, BRAF and phosho-ERK1/2 immunostaining in lung tumors from *C/BRAF** mice. *D*, Western blot analysis of phospho-AKT and phospho-ERK1/2 levels in whole lung lysates from nontransgenic mice or *C/BRAF** mice without (−) or with (+) doxycycline and/or followed doxycycline withdrawal (+/−). β-Actin serves as a loading control.

Table 1. Summary of lung cancer incidence in C/BRAF* mice

Genotype	On doxycycline	Cancer incidence, *n* (%)
C/BRAF*	Yes	41/44 (93)
C/BRAF*	No	0/7 (0)
BRAF*	Yes	0/10 (0)

expression was detectable in the *C/BRAF** mouse lungs without doxycycline treatment (Fig. 1*A*). After doxycycline administration for 12 weeks, its expression was readily induced and returned to an undetectable level after 2 weeks of doxycycline withdrawal (Fig. 1*A*). To determine the relative expression level of transgene, RT-PCR and immunoblotting were done to detect the total BRAF levels including both endogenous and transgene *BRAF**. The results showed that there were no discernible differences in total BRAF expression at either RNA or protein level between the nontransgenic mice and *C/BRAF** mice with or without doxycycline treatment, suggesting transgene expression is low compared with endogenous mouse BRAF (Supplementary Fig. S2). However, we cannot exclude that a small percentage of cells express high amounts of BRAF* and that a high expression of BRAF* is necessary to transform lung epithelial cells.

We next did serial histologic analysis on the lungs from *C/BRAF** mice after doxycycline administration at various time points (6, 10, 13, and 16 weeks). Up to an age of 30 weeks, all *C/BRAF** mice without doxycycline treatment or *BRAF** monotransgenic mice with doxycycline treatment showed normal lung histology with no evidence of malignancy (Table 1). In contrast, the bitransgenic mice began to develop adenomas with bronchioloalveolar carcinoma features after 6 weeks of doxycycline treatment (Table 1). All bitransgenic mice receiving doxycycline developed adenocarcinoma with acinar, solid, and bronchioloalveolar carcinoma–like features after 16 weeks of treatment (Fig. 1*B*), phenotypically resembling human adenocarcinomas. As expected, the tumors were surfactant protein C positive and Clara cell marker negative, indicating a type II pneumocyte origin (data not shown). All tumors stained positive for both BRAF and phospho-ERK1/2, suggesting that expression of BRAF* activated ERK1/2 during lung tumorigenesis (Fig. 1*C*). Consistent with previous studies (4, 5), we observed a high baseline level of phospho-ERK1/2 in normal lungs by immunoblotting (Fig. 1*D*). Doxycycline treatment only slightly increased levels of phospho-ERK1/2 in whole lung lysates (Fig. 1*D*). This could potentially be due to the relative small percentage of BRAF*-expressing cells. Intriguingly, doxycycline withdrawal dramatically and consistently decreased the phospho-ERK1/2 level to a degree even lower than that seen in normal lung lysates (Fig. 1*D*). These data indicate that down-regulation of BRAF* by doxycycline withdrawal results in ERK1/2 inactivation not only in tumor cells but also in the majority of normal cells through some unknown interactions. In contrast, the phospho-AKT level was not significantly altered throughout all different conditions of doxycycline administration (Fig. 1*D*). These data indicate that expression of BRAF* induces lung tumor formation mainly through activation of the MAPK pathway.

Expression of BRAF* is essential for tumor maintenance. To determine the role of BRAF* in lung tumor maintenance, we abrogated BRAF* expression in tumor-bearing mice through doxycycline withdrawal. After 2 weeks of doxycycline withdrawal, the average tumor burden was reduced by $73 \pm 19\%$ according to MRI analysis (Fig. 2*A*; Supplementary Table S1). Histologically, there was evidence of dramatically reduced tumor burden (Fig. 2*A, right*). There were focal areas of interstitial fibrosis, mild chronic inflammation, and reactive epithelial changes that likely represent areas of tumor regression (Fig. 2*A, right*). In addition, we found areas of increased numbers of intra-alveolar macrophages with strongly eosinophilic cytoplasm; these areas likely represent a postobstructive change and there was no evidence of malignancy in these foci (data not shown). In some cases, this inflammation associated with tumor regression may persist for up to 5 weeks of doxycycline withdrawal and may still appear in MRI analysis (Supplementary Fig. S3). It is important to note these areas histologically because they will manifest as consolidation on MRI. Imaging may therefore underestimate the degree of tumor regression. The tumors did not recur after 5 or 7 weeks of doxycycline withdrawal by histologic analysis (data not shown). To study early changes associated with oncogene deinduction, tumor-bearing mice were sacrificed after 3 days of doxycycline withdrawal. Immunostaining of lung tumors indicated a dramatic decrease of both phospho-MEK1/2 and phospho-ERK1/2 levels that co-occurred with decreased levels of cyclins D1, D2, and D3 (Fig. 2*C*). Immunoblotting analysis confirmed that phospho-ERK1/2 levels, but not phospho-AKT levels, dramatically decreased in the lung tumor lysates after 3 days of deinduction of BRAF* expression through doxycycline withdrawal (Figs. 1*D* and 2*D*). This indicates that inhibition of the MAPK pathway rather than suppression of the AKT pathway is associated with lung tumor regression. Tumor regression was caused by growth arrest and induction of apoptosis of tumor cells as deinduction of BRAF* expression was accompanied by a significant increase (24-fold) of terminal deoxyribonucleotidyl transferase–mediated dUTP nick end labeling (TUNEL)–positive cells and by a substantial decrease of proliferating cell nuclear antigen (PCNA)–positive cells (53%; Fig. 3). These data indicate that deinduction of BRAF* decreases the level of constitutively activated MAPK pathway and leads to lung tumor regression associated with growth arrest and apoptosis.

Pharmacologic inhibition of the MAPK pathway by the MEK 1/2 inhibitor CI-1040 induces tumor regression in *C/BRAF mice.** To investigate the role of BRAF*-MEK-ERK pathway in tumor maintenance, the MEK1/2 inhibitor CI-1040 was used to block the activation of MAPK pathway. Tumor-bearing *C/BRAF** mice were daily treated with the inhibitor and serially analyzed by MRI to document tumor burden. CI-1040 was given orally 150 mg/kg twice a day, which is a dose commonly used to block MAPK pathway activation in xenograft mouse models (13, 14). All mice were kept on doxycycline throughout the CI-1040 treatment. After 2 weeks of CI-1040 treatment, dramatic tumor regression was observed by MRI with an average of $62 \pm 11\%$ tumor reduction (Fig. 2*B*; Supplementary Table S2). Consistently, histologic analysis showed a pronounced tumor regression. There were very few tumor remnants representative of areas of tumor regression after 2 weeks of treatment (Fig. 2*B*). After 3 weeks of treatment, lung specimens showed essentially normal histology (Supplementary Table S2 and data not shown).

Both immunostaining and immunoblotting analyses were done to assess the early biochemical changes after 3 days of CI-1040 treatment. Effective inhibition of both phospho-MEK1/2 (Fig. 2*C*)
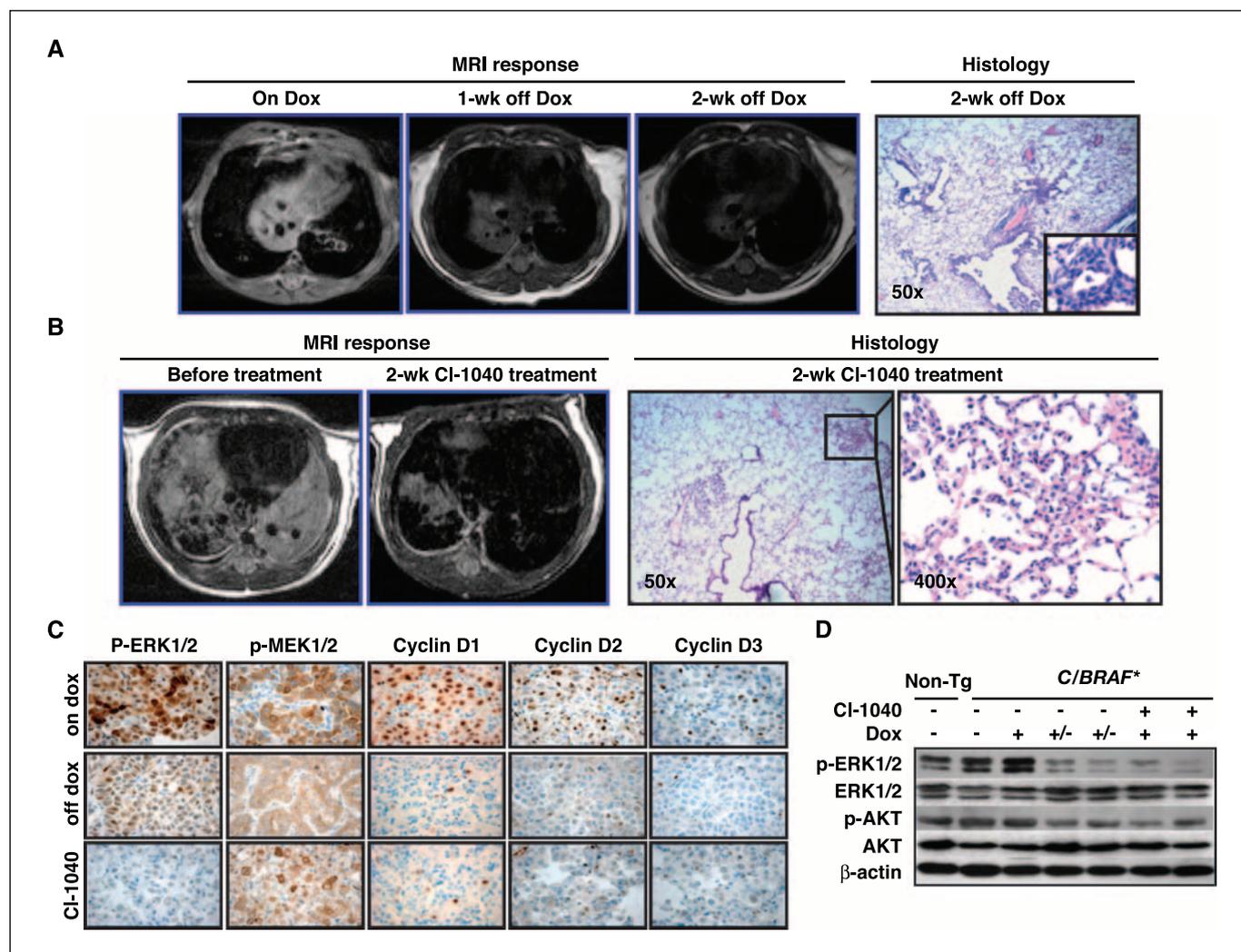
Figure 2. Analyses of lung tumor regression through either deinduction of BRAF* expression or MEK inhibitor CI-1040 treatment in *C/BRAF** mice. *A, C/BRAF** mice were given doxycycline diet for 14 wk and the food was replaced with normal diet for 2 wk. The mice were MRI scanned before and after changing diet at the indicated time points (*left*). H&E staining of mouse lung tissues after 2 wk of doxycycline withdrawal; high-magnification view showing the tumor remnants (*right*). *B, C/BRAF** mice were MRI scanned before and after CI-1040 treatment for 2 wk (*left*). H&E staining of the mouse lung tissues illustrated the tumor remnants associated with inflammation (*right*). *C,* reduction of phospho-ERK1/2 and phospho-MEK1/2 levels was concurrent with a decrease of cyclin D1, cyclin D2, and cyclin D3 expression in lung tumors after 3 d of either doxycycline withdrawal or CI-1040 treatment. *D,* blockage of phospho-ERK1/2 but not phospho-AKT was observed in the whole lung lysates from *C/BRAF** mice after 3 d of either doxycycline withdrawal or CI-1040 treatment. β-Actin serves as a loading control.

and phospho-ERK1/2 (Fig. 2*C* and *D*) was observed after CI-1040 treatment, similar to the extent seen after deinduction of BRAF* expression. This inhibition of MAPK pathway is concurrent with a decrease of cyclin D1, cyclin D2, and cyclin D3 protein levels (Fig. 2*C*). Similar to the results obtained with deinduction of transgene expression, we did not observe a dramatic change in protein levels of phospho-AKT on treatment with CI-1040, corroborating the notion that AKT may not be involved in this tumor maintenance. Tumor regression induced by CI-1040 treatment was accompanied by cell cycle arrest and induction of apoptosis illustrated by an increase of TUNEL-positive cells (7-fold) and a decrease of PCNA-positive cells (67%; Fig. 3). No discernible effect of CI-1040 treatment on cellular proliferation and apoptosis was seen in the normal lung epithelial cells from nontransgenic mouse controls (Supplementary Fig. S4). These observations support an essential role of the MAPK pathway in tumor maintenance in BRAF* lung tumors.

CI-1040 induces tumor shrinkage in murine lung tumors driven by oncogenic *KRas*. To determine whether tumor maintenance in tumors driven by an oncogenic allele of *KRas* (G12D, *KRas**) is also dependent on activation of the MAPK pathway, we made use of the previously established murine *KRas**-mutant lung tumor mouse model (12). After induction of *KRas** for more than 8 weeks, the bitransgenic *CCSP-rtTA/Tet-op-KRas** (short as *C/KRas**) mice developed lung adenocarcinomas. After 2 weeks of CI-1040 treatment, MRI analysis showed a dramatic decrease of tumor burden (53 ± 5%; Fig. 4*A*; Supplementary Table S3). Histologic analysis showed that four of five treated mice were completely free of tumor and only one mouse still contained some tumor nodules with tumor remnants, in comparison with the large tumor burden in control groups (Fig. 4*B*). The lung tumors exhibited a strong decrease of phospho-ERK1/2 level without any change of phospho-AKT level (Fig. 4*C* and data not shown). Tumor shrinkage was likely due to growth

arrest and induction of apoptosis as a dramatic increase of TUNEL-positive cells (7-fold) and a 58% decrease of PCNA-positive cells were observed after 3 days of CI-1040 treatment (Fig. 4D). Thus, tumor maintenance in KRas*-driven lung tumors *in vivo* may be dependent on continuous activation of the MAPK pathway.

Discussion

Previous studies have shown that overexpression of either *wt* or activated c-Raf-1 drives lung adenomas (15). In contrast, our data presented here show that expression of the BRAF V600E mutant induced lung adenocarcinomas *in vivo*, which are similar to KRas* tumors and phenotypically resembled human adenocarcinoma (12).

Tumor initiation and maintenance in BRAF* mice were strictly dependent on activation of the MAPK pathway. Importantly, in contrast to lung tumors with genetic lesions in *EGFR* alleles, we found no evidence for crucial involvement of the AKT pathway in tumor initiation and maintenance in lung tumors with *BRAF* mutation. The exquisite dependency on the MAPK pathway may provide a robust rationale for the use of MAPK pathway inhibitors in these settings, whereas inhibitors of AKT or phosphatidylinositol 3-kinase might be less effective as previous reported (9). Consequently, therapeutic inhibition of the MAPK pathway by CI-1040 treatment induced dramatic tumor shrinkage in our murine BRAF-mutant lung tumors, a process that was paralleled by dephosphorylation of ERK1/2, growth arrest, and induction of apoptosis. In contrast, no discernable apoptosis was observed after 21 days of CI-1040 treatment of the c-Raf mutant–driven lung adenomas (16). One plausible explanation is that apoptosis induced by CI-1040 treatment might occur at a much earlier time point because our TUNEL experiment was done after 3 days of CI-1040 treatment. Interestingly, CI-1040 also proved effective in treatment of lung tumors driven by the oncogenic allele of *KRas*. Thus, mutations in BRAF and KRAS converge on activation of the MAPK pathway in lung tumor initiation and tumor maintenance, implying this pathway as an attractive therapeutic target in patients with BRAF and KRAS mutant lung tumors.

Previous studies in xenograft models using human melanoma or colon cancer cell lines have proved that inhibition of MAPK pathway by CI-1040 or other MEK inhibitor is effective in cancer treatment (17, 18). However, these experiments were associated with tumor growth arrest instead of tumor regression (17, 18). In contrast, we observed a much profound tumor regression associated with induction of apoptosis in lung tumors with either *BRAF* or *KRas* mutation after CI-1040 treatment. This may be due to the different genetic requirements for tumor maintenance in different tumor lineages. Another explanation might be that human cancer cell lines harbor additional genetic lesions, some of which may dilute the proapoptotic effects of CI-1040 observed in this study. Further work is warranted to identify these genetic events that potentially serve as targets for combinational therapy with MAPK inhibition. Nonetheless, our data have validated the MAPK pathway as a good therapeutic target in ∼30% of non–small-cell lung cancers harboring either *KRAS* or *BRAF* mutations.

Recently, results from phase I and phase II clinical trials of CI-1040 have been reported in treatment of human cancers including non–small-cell lung cancer (19, 20). In phase I trial of 66 patients with different human cancers including non–small-cell lung cancer, only one pancreatic cancer patient achieved partial response and 19 patients achieved stable disease lasting 5.5 months on average (19, 20). Similarly, only stable disease, but no objective response, was observed in 8 of 67 patients in phase II trials (19, 20). Although the results of these trials are somewhat disappointing, it is important to note that no information on the different oncogenic mutation status was provided (19). Furthermore, the ineffectiveness of CI-1040 could be attributed to its instability and low potency *in vivo* against MEK inhibition, which may be associated with inefficient inhibition of MAPK pathway (19). Recently, a second-generation MEK inhibitor, PD 0325901, is under clinical development (19). In contrast to CI-1040, PD 0325901 exhibits a much higher potency against MEK, much improved oral bioavailability, and longer duration of target suppression (19). This newer second generation of MEK inhibitors
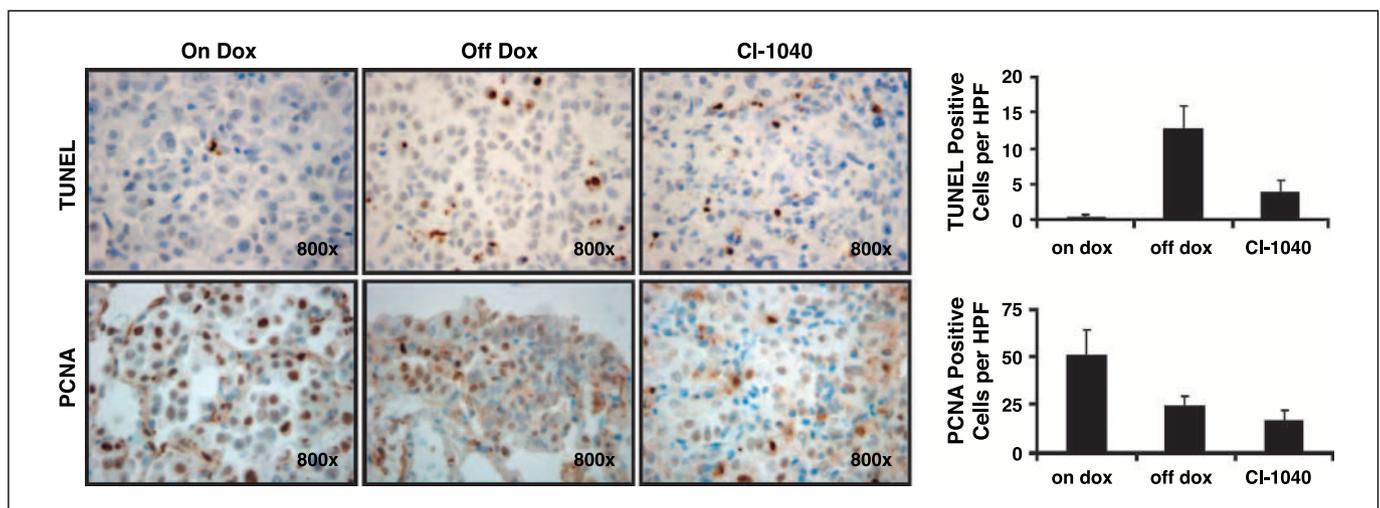

Figure 3. Tumor regression induced by either doxycycline withdrawal or CI-1040 treatment is associated with apoptosis. TUNEL and PCNA immunohistochemical staining were done on mouse lung tissues before and after 3 d of either doxycycline withdrawal or CI-1040 treatment. *Columns,* average number of TUNEL- or PCNA-positive cells counted from >50 high-power fields (*HPF*); *bars,* SD. $P < 0.05$, on-doxycycline group (*on dox*) compared with either off-doxycycline group (*off dox*) or CI-1040 treatment group in both graphs (Student's *t* test).
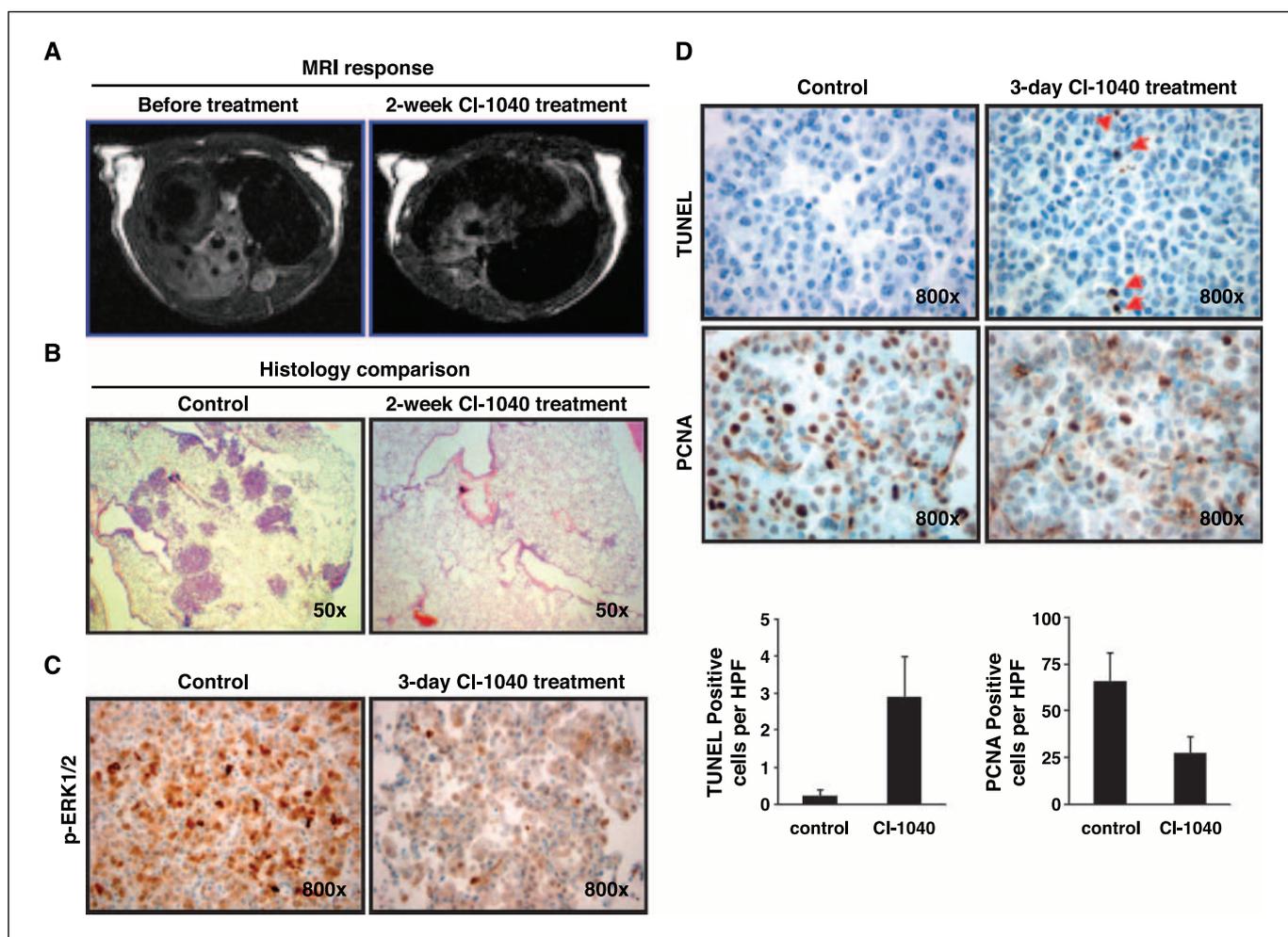
Figure 4. CI-1040 treatment leads to lung tumor regression associated with tumor growth arrest and apoptosis in *C/KRas** mice. *A, C/KRas** mice were given doxycycline diet for >8 wk and food was then replaced with normal diet for 2 wk. Mice were MRI scanned before and after changing diet at the indicated time points. *B,* histologic illustration of lung tumors with or without 2 wk of CI-1040 treatment in *C/KRas** mice. *C,* three days of CI-1040 treatment dramatically decreased the phospho-ERK1/2 levels in lung tumors, shown by immunostaining; *D,* three days of CI-1040 treatment was associated with dramatic increase of TUNEL-positive cells and decrease of PCNA-positive cells. *Columns,* average number of TUNEL- or PCNA-positive cells counted from >50 high-power fields; *bars,* SD. $P < 0.05$, control compared with the CI-1040 treatment group (Student's *t* test).

may prove clinically effective in patients with BRAF and KRAS mutant tumors.

In summary, we have shown that mutations in *KRAS* and *BRAF* found to occur in a mutually exclusive fashion in human lung cancer share a common effector pathway in tumor maintenance *in vivo*. These observations thereby unveil a common therapeutic vulnerability to MEK inhibitors in BRAF and KRAS mutant human lung tumors. Lastly, these two lung cancer mouse models can serve as platforms for *in vivo* validation of therapeutics that specifically target the RAS/RAF/MAPK pathways.

References

1. Beeram M, Patnaik A, Rowinsky EK. Raf: a strategic target for therapeutic development against cancer. J Clin Oncol 2005;23:6771–90.
2. Davies H, Bignell GR, Cox C, et al. Mutations of the BRAF gene in human cancer. Nature 2002;417:949–54.
3. Emuss V, Garnett M, Mason C, Marais R. Mutations of C-RAF are rare in human cancer because C-RAF has a low basal kinase activity compared with B-RAF. Cancer Res 2005;65:9719–26.
4. Ji H, Zhao X, Yuza Y, et al. Epidermal growth factor receptor variant III mutations in lung tumorigenesis and sensitivity to tyrosine kinase inhibitors. Proc Natl Acad Sci U S A 2006;103:7817–22.
5. Ji H, Li D, Chen L, et al. The impact of human EGFR kinase domain mutations on lung tumorigenesis and *in vivo* sensitivity to EGFR-targeted therapies. Cancer Cell 2006;9:485–95.
6. Politi K, Zakowski MF, Fan PD, Schonfeld EA, Pao W, Varmus HE. Lung adenocarcinomas induced in mice by mutant EGF receptors found in human lung cancers respond to a tyrosine kinase inhibitor or to down-regulation of the receptors. Genes Dev 2006;20:1496–510.

7. Sordella R, Bell DW, Haber DA, Settleman J. Gefitinib-sensitizing EGFR mutations in lung cancer activate anti-apoptotic pathways. Science 2004;305:1163–7.

8. Lim KH, Counter CM. Reduction in the requirement of oncogenic Ras signaling to activation of PI3K/AKT pathway during tumor maintenance. Cancer Cell 2005;8:381–92.

9. Wislez M, Spencer ML, Izzo JG, et al. Inhibition of mammalian target of rapamycin reverses alveolar epithelial neoplasia induced by oncogenic K-ras. Cancer Res 2005;65:3226–35.

10. Sebolt-Leopold JS, Herrera R. Targeting the mitogen-activated protein kinase cascade to treat cancer. Nat Rev Cancer 2004;4:937–47.

11. Mercer K, Giblett S, Green S, et al. Expression of endogenous oncogenic V600EB-raf induces proliferation and developmental defects in mice and transformation of primary fibroblasts. Cancer Res 2005;65:11493–500.

12. Fisher GH, Wellen SL, Klimstra D, et al. Induction and apoptotic regression of lung adenocarcinomas by regulation of a K-Ras transgene in the presence and absence of tumor suppressor genes. Genes Dev 2001;15:3249–62.

13. Adnane L, Trail PA, Taylor I, Wilhelm SM. Sorafenib (BAY 43-9006, Nexavar((R))), a dual-action inhibitor that targets RAF/MEK/ERK pathway in tumor cells and tyrosine kinases VEGFR/PDGFR in tumor vasculature. Methods Enzymol 2005;407:597–612.

14. McDaid HM, Lopez-Barcons L, Grossman A, et al. Enhancement of the therapeutic efficacy of Taxol by the mitogen-activated protein kinase kinase inhibitor CI-1040 in nude mice bearing human heterotransplants. Cancer Res 2005;65:2854–60.

15. Kerkhoff E, Fedorov LM, Siefken R, Walter AO, Papadopoulos T, Rapp UR. Lung-targeted expression of the c-Raf-1 kinase in transgenic mice exposes a novel oncogenic character of the wild-type protein. Cell Growth Differ 2000;11:185–90.

16. Kramer BW, Gotz R, Rapp UR. Use of mitogenic cascade blockers for treatment of C-Raf induced lung adenoma *in vivo*: CI-1040 strongly reduces growth and improves lung structure. BMC Cancer 2004;4:24.

17. Sebolt-Leopold JS, Dudley DT, Herrera R, et al. Blockade of the MAP kinase pathway suppresses growth of colon tumors *in vivo*. Nat Med 1999;5:810–6.

18. Solit DB, Garraway LA, Pratilas CA, et al. BRAF mutation predicts sensitivity to MEK inhibition. Nature 2006;439:358–62.

19. Rinehart J, Adjei AA, Lorusso PM, et al. Multicenter phase II study of the oral MEK inhibitor, CI-1040, in patients with advanced non-small-cell lung, breast, colon, and pancreatic cancer. J Clin Oncol 2004;22:4456–62.

20. Lorusso PM, Adjei AA, Varterasian M, et al. Phase I and pharmacodynamic study of the oral MEK inhibitor CI-1040 in patients with advanced malignancies. J Clin Oncol 2005;23:5281–93.

Mutations in BRAF and KRAS Converge on Activation of the Mitogen-Activated Protein Kinase Pathway in Lung Cancer Mouse Models

Hongbin Ji, Zhenxiong Wang, Samanthi A. Perera, et al.

Updated version	Access the most recent version of this article at: http://cancerres.aacrjournals.org/content/67/10/4933
Supplementary Material	Access the most recent supplemental material at: http://cancerres.aacrjournals.org/content/suppl/2007/05/11/67.10.4933.DC2

Cited articles	This article cites 20 articles, 12 of which you can access for free at: http://cancerres.aacrjournals.org/content/67/10/4933.full.html#ref-list-1
Citing articles	This article has been cited by 37 HighWire-hosted articles. Access the articles at: /content/67/10/4933.full.html#related-urls

E-mail alerts	Sign up to receive free email-alerts related to this article or journal.
Reprints and Subscriptions	To order reprints of this article or to subscribe to the journal, contact the AACR Publications Department at pubs@aacr.org.
Permissions	To request permission to re-use all or part of this article, contact the AACR Publications Department at permissions@aacr.org.